DISCRETE AND CONTINUOUS
DYNAMICAL SYSTEMS SERIES S
Volume **12**, Number **4&5**, August & September **2019**

doi:10.3934/dcdss.2019086

pp. **1251–1264**

AUTOMATIC TRACKING AND POSITIONING ALGORITHM FOR MOVING TARGETS IN COMPLEX ENVIRONMENT

Rong Liu

Unmanned Aerial Vehicle Research Institute, Nanjing University of Aeronautics and Astronautics, Nanjing 210016, China

Saini Jonathan Tishari

Department of Mathematics UMBA
University of Mostaganem Algeria, Algeria

Abstract. Nowadays, when moving targets are located in complex environment, the positioning algorithm takes longer time, and the result is not consistent with the actual positioning of the moving target, which has the problem of low positioning efficiency and inaccurate positioning results. In this paper, a moving target automatic tracking and positioning algorithm is proposed in the complex environment, which establishes the geodetic coordinate system and the space rectangular coordinate system, and completes the transformation between the geodetic coordinate system and the rectangular coordinate system, so as to improve the accuracy of the positioning result. The signal is rebuilt and the MIMO radar positioning model is used to complete the automatic tracking and positioning of the moving target in complex environment, to reduce the time consuming. The experimental results show that the proposed method can quickly and accurately track and locate the moving target in complex environment.

1. **Introduction.** With the development of the level of science and technology, the means of positioning also changed [15]. At a time when the level of science and technology is low, it relies mainly on the investigators do the on-the-spot investigation or close range investigation to complete the positioning of the enemy or the threat target [5]. In this period, the way of investigation can give full play to people's activity role. Even in the modern war with rapid development of science and technology, it is still an important way of investigation [22]. However, because human subjectivity will bring greater errors and combining with the hard working conditions and low efficiency, in most cases, people can not get close to the threat targets, which brings many difficulties to the investigation [18, 20]. With the progress of science and technology, it has the optical instrument, people can use it to observe the distant target [12]. However, optical instruments depend on the light emitted by the observed target or the light emitted by other illuminating objects to observe the reflected light of the target, which limits the conditionse.g. it can not observe by the optical instrument in the night; in the daytime, in the cloud, rain, fog, snow and other poor weather conditions, it greatly reduces the ability of

2010 *Mathematics Subject Classification.* 51M35.
Key words and phrases. Moving target, automatic tracking, location algorithm.
* Corresponding author: Rong Liu.

observation; in good weather conditions, the human eye through an optical instrument capable of observing the distance is very limited [21, 25]. After entering the era of information, this kind of mechanical observation and positioning obviously can not meet the requirement of the application of [16]. With the development and application of radar during World War II, in late 1930s, the active radar system began to detect a few thousand to thousand meters, become a basic tool for modern military war [17]. Radar is different from optical instruments. It launches electromagnetic waves to detect targets. As long as targets can reflect the electromagnetic waves emitted by them, it is possible to achieve observations, and detect long distance target no matter during the day or at night [2, 3, 7–11, 23]. The radar system can get the distance between radar and target by measuring the time delay between the transmitted wave and the echo. The angle of the target is measured by the directivity of the antenna, and the velocity of the target can be calculated by the change rate of the transmitted wave and the carrier frequency of the echo [24]. When the moving target positioning algorithm is used to locate the moving target in complex environment, the positioning time is longer. The location result is not consistent with the actual location of the moving target. It has the problem of low location efficiency and inaccurate location result [1, 4, 6, 13, 14, 19, 26, 27]. In this paper, an automatic tracking and positioning algorithm for moving targets in complex environment is proposed in this paper in order to solve the above problems.

2. camera model and coordinate transformation.

2.1. Camera model.

Optical imaging is a small hole imaging model based on the theory of perspective projection. If the lens distortion is taken into account, it can be divided into nonlinear and linear models. Due to the advantages of easy understanding and calibration of projective geometry, radiation geometry and Euclidean geometry, the geometric transformation theory can be used to establish approximate linear model. The projection of object to the imaging plane in three-dimensional space is the imaging model. The ideal projection model is the model of center projection in optics, namely the linear model, which is the camera model of all the scenery imaging onto the plane through the optical axis of the camera, also known as pin hole model. In the pinhole model, it is assumed that the reflected light on the surface of the object is projected onto the image plane through a pinhole to

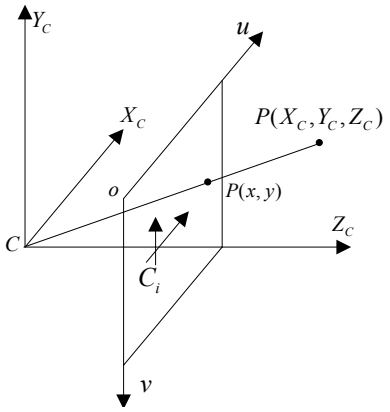

FIGURE 1. Model of pin hole imaging

satisfy the linear propagation condition of the light. The lens transformation model based on pin hole imaging is the most basic model, and it is also the most common ideal model. The camera pinhole model mainly includes the photo center (the projection center), an imaging surface and the optical axis, as shown in Figure 1. Among them, (X_C, Y_C, Z_C) is the camera coordinate system; (u, o, v) is the image pixel coordinate system, $p(x, y)$ is the image point coordinate, and $p(X_C, Y_C, Z_C)$ is the coordinate of the camera in the geodetic coordinate system.

Based on the imaging principle and imaging characteristics of a camera, the brightness of every point on the photo reflects the intensity of the reflected light of the corresponding points on the surface of the object, that is, the location of the image points on the image, which is related to the geometric position of the corresponding points on the surface of the space object. The geometric position relation is determined by the camera geometric model. The vertical distance CO between camera optical center C to the photograph is main distance of camera; $CO = f, f$ is the focal length and point O is principal point of photograph. The reason why the camera is made is that the midpoint O of the photo does not coincide with the photo's main point o'. There is a slight deviation x_0, y_0. This error is called the main point deviation, and (x_0, y_0, f) is called the intrinsic parameter of camera.

To achieve the solution from the coordinates of image points to the coordinates of the target points, it first needs to determine the spatial position and direction of the camera beam at the moment of exposure, that is, the position and orientation of the camera coordinate system in the geodetic coordinate system. The position of the camera coordinate system in the geodetic coordinate system is determined by the three-dimensional coordinate (X_C, Y_C, Z_C) of the projection center in the geodetic coordinate system, that is, the line element. The azimuth is determined by the azimuth element $(\varphi, \omega, \kappa)$ of the camera coordinate system in the geodetic coordinate system. (X_C, Y_C, Z_C) is used to determine the position of the camera φ, ω, κ, is used to determine the orientation of camera, where, the declination angle φ and the obliquity ω can determine the direction of mail optical axis, and the rotation angle κ can determine the orientation of photos in the image plane. The angles of the angle system φ, ω, κ are defined as shown in Figure 2, of which (X_W, Y_W, Z_W) is the WGS-84 coordinate system; (X_C, Y_C, Z_C) is the camera coordinate; (u, v, w) is the assistant camera coordinate system; (x, o, y) is the image's physical coordinate system; The drift angle φ is the angle between the projection of main optical axis on the XZ plane and the axis Z. To observe along the positive direction of Y axis, the counter clockwise is the positive direction; rotation angle k is the angle between the plane composed of the main axis and Y axis and image plane intersection and 18 axis and the intersection of image plane and the Y axis of Cartesian coordinate system, in clockwise direction, starting from the intersection, counterclockwise is positive direction; the obliquity ω is the angle of the main axis and its projection on the plane XZ. it is defined that along with the positive direction of x axis to observe to the origin of the coordinate, counter clockwise is specified as the positive direction.

2.2. **The establishment of the coordinate system and the coordinate transformation.** Image coordinate system is a rectangular coordinate system defined on two-dimensional images. It is divided into two types: physical coordinate system based on physical length and pixel coordinate system in pixels. Customarily, the origin of the image physical coordinate is defined at the center of the image. The original point of the image pixel coordinate system is generally defined at the top

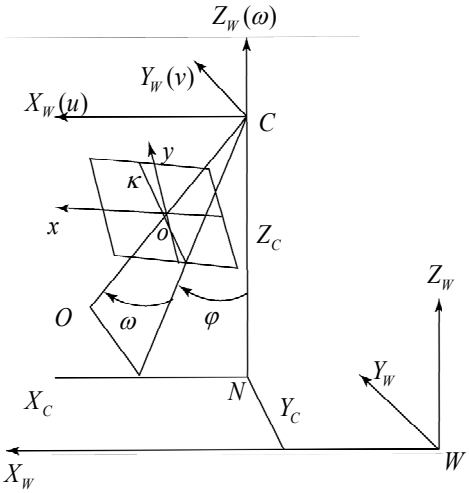

FIGURE 2. Diagram of corner system φ, ω and κ

left corner of the image. The origin of image physical coordinate system is the intersection point between lens optical axis and imaging plane. Because of the reason of camera manufacture, the central point of image does not coincide with the intersection point. x axis and y axis are parallel to the x axis and y axis of the camera coordinate system, which is a plane right angle coordinate system, the unit is millimeter. Image pixel coordinate system is a plane rectangular coordinate system fixed on the image in pixels. Its origin is located at the upper left corner of the image. x_f and y_f are parallel to the x axis and y axis of the physical coordinate system. For digital images, they are row and column directions respectively. For the convenience of calculation, in this paper, the physical coordinate system of image, that is, the plane rectangular coordinate system xoy is selected, the position of image points on the photo plane is decided by the plane coordinate (x, y) in the image plane. The conversion relation between the image physical coordinate system $(r, c)_{pixel}$ and the image pixel coordinate $(X_i, Y_i)_{mm}$ is as follows:

$$\begin{cases} r = X_i S_x + r_0 \\ c = Y_i S_y + c_0 \end{cases} \tag{1}$$

Where, (r_0, c_0) is the intersection point coordinate of the image plane and the optical axis, and S_x and S_y are the magnification coefficients of the camera CCD photosensitive component in the x axis and the y axis direction.

The geodetic coordinate is converted to spatial Cartesian coordinate as:

$$\begin{cases} X = (N + H)\cos B \cos L \\ Y = (N + H)\cos B \sin L \\ Z = \left[N(1 - e^2) + H\right]\sin B \end{cases} \tag{2}$$

The spatial Cartesian coordinate is converted to geodetic coordinate as.

$$\begin{cases} L = \arctan\left(\dfrac{Y}{X}\right) \\ B = \arctan\left(\dfrac{Z + Ne^2 \sin B}{\sqrt{X^2 + Y^2}}\right) \\ H = \dfrac{\sqrt{X^2 + Y^2}}{\cos B} - N \end{cases} \tag{3}$$

Where, N is the curvature radius of the ellipsoid unitary ring, $N = a/\sqrt{1 - e^2 \sin^2 B}$, e is the first eccentricity of the ellipsoid, and a is the ellipsoidal short half axis radius.

If the movement of the origin of the different coordinate system $(\Delta X, \Delta Y, \Delta Z)$ is known, it can use the next formula to calculate the coordinates.

$$\begin{cases} \Delta B'' = \dfrac{1}{M \sin 1''} \left[(a\Delta e^2 + e^2 \Delta a) \sin B_1 \cos B_1\right] \\ \Delta L'' = \dfrac{1}{N \cos B_1 \sin 1''} (\cos L_1 \Delta Y - \sin L_1 \Delta X) \end{cases} \tag{4}$$

Where, B_1 and L_1 are the latitude and longitude of the original coordinate; $M = a(1 - e^2)/(1 - e^2 \sin^2 B_1)^{3/2}$ is the curvature radius of the meridian circle of original coordinate system; $N = a/(1 - e^2 \sin^2 B_1)^{1/2}$ the curvature radius of the prime vertical of original coordinate system; $\Delta a = a_2 - a_1, a_1$ is the elliptical semimajor axis of original coordinate; a_2 is the elliptical semimajor axis of new coordinate system.

$$e^2 = (2 - 2c_1)(c_2 - c_1) \tag{5}$$

c_1 is the ellipticity of original coordinate; e^2 is the eccentricity of ellipse square of original coordinate; $1 - \sin 1'' = 206264.8062$. After $\Delta B''$ and $\Delta L''$ are solved, the coordinate values in the new form of geodetic coordinate system are as:

$$\begin{cases} B_2 = B_1 + \Delta B'' \\ L_2 = L_1 + \Delta L'' \end{cases} \tag{6}$$

Where, B_2 and L_2 are the latitude and longitude of new coordinate.

3. **Automatic tracking and positioning algorithm for moving target.**

3.1. **Reconstruction of signal.** The one dimensional real value's discrete time signal $x \in R^N$ with a length of N is taken as an example, that is, $x = [x(1), x(2), \ldots, x(N)]$. Let $\Psi = [\varphi_1, \varphi_2, \ldots, \varphi_N]$ be a set of bases on R^N space, where each element $\varphi_i (i = 1, 2, \ldots, N)$ represents a column vector of $N + 1$. Any signal in the space can be expressed in linear combination of Ψ, that is:

$$x = \Psi s = \sum_{i=1}^{N} \varphi_i s_i = \varphi_1 s_1 + \varphi_2 s_2 + \cdots + \phi_N s_N \tag{7}$$

In formula (7), s is a $N \times 1$ column vector consisting of projection coefficient $s_i = < X, \Psi_i >$. To some extent, x and s are equivalent, and are different forms of representation in different domains. If the coefficient s of the signal x on the base Ψ has only K non zero values, it is called the signal x has K sparsity.

The sparse approximation of signals is essentially two tasks: first, according to the structure of the original signal, the best atoms are selected from the given atomic library; then the best combination is selected from the best atoms. For a given set

$D = \{g_i, i = 1, 2, \ldots, I\}$, the atom g_i is the unit vector of the entire Hilbert space $H = R^N$. For any signal $f \in H$, it needs to select m atoms from the set D to make m set of approximations to the signal.

$$f_m = \sum_{\gamma \in I_m} c_\gamma g_\gamma \tag{8}$$

Where, I_m is the subscript set of the atom g_γ, and c_γ is the coefficient of the sparse decomposition. The approximation error is defined as follows:

$$\sigma_m = \inf_{f_m} \|f - f_m\| \tag{9}$$

In order to meet the requirement of sparsity, under the condition of satisfying formula (8), it is necessary to select a set of atoms corresponding to the least zero decomposition coefficients from various combinations, which solves the problem of sparse representation of signals. This problem is mathematically expressed as:

$$\min \|< f, g_i >\| \quad s.t \quad f = \sum_{i=0}^{I-1} < f, g_i > g \tag{10}$$

Assuming that the signal x is a compressible signal with a length of N, and its sparsity is expressed as:

$$x = \Psi s \tag{11}$$

s is a sparse vector of signal x. The measurement vector y of the length of M is obtained by the original signal x projected to the $M \times N(M < N)$ dimensional measurement matrix Φ.

$$y = \Phi x \tag{12}$$

The formula (11) is brought into the formula (12):

$$y = \Phi \Psi s = \Theta s \tag{13}$$

In formula (13), $\Theta = \Phi\Psi$, which is the $M \times N$ matrix, is called the perception matrix. For any K sparse signal x, if there is a minimum constant $\varepsilon_k \in (0, 1)$, it satisfies:

$$(1 - \varepsilon_k) \|x_T\|_2^2 \leq \|\Theta_T x_T\|_2^2 \leq |(1 + \varepsilon_k) \|x_T\|_2^2 \tag{14}$$

Then, it is called the perception matrix Θ to satisfy the RIP property. Where, $T \subset \{1, \ldots, N\}, |T| \leq K$, and Θ_T are the $K \times |T|$ dimensional submatrices of the related columns that have been subscribed to T in matrix Θ.

If the observation matrix Φ is incoherent with the sparse transform base Ψ, then $\Theta = \Phi\Psi$ can greatly satisfy the RIP property. The coherence coefficients are defined as:

$$\mu = \max_{i \neq j} |< \phi_i, \Psi_j >| \tag{15}$$

In formula (15), φ_i and Ψ_j are column vectors of matrix φ_i and Ψ, respectively. The size of the coherence coefficient μ indicates the intensity of the coherence between the matrices. The lower the correlation between the two (that is, the smaller the μ is) is, the less the measured value is required.

The signal x is a N dimensional discrete signal, that is, $x = [x_1, x_2, \ldots, x_N]$, and its $l-$norm is:

$$\|x\|_l = \left(\sum_{i=1}^{N} |x_i"|^l \right)^{1/l} \tag{16}$$

When $l = 0$, the 0- norm $\|x\|_0$ of the obtained signal x indicates the number of non zero terms in the vector x, that is, the sparsity of the signal. 0- norm (l_0 norm) fully reflects the number of non zero elements in the signal, and makes the result as sparse as possible. So the most direct signal reconstruction method is to solve the optimization problem of the minimum l_0 norm.

$$\widehat{s} = \arg\min \|x\|_0 \quad s.t. \quad y = \Phi x \tag{17}$$

Generally, the signal is not strictly sparse, but it is compressible. For such a signal, the problem of the underdetermined equation of formula (13) is transformed into the problem described in formula (18).

$$\widehat{s} = \arg\min \|s\|_0 \quad s.t. \quad y = \Phi\Psi s = \Theta s \tag{18}$$

The solution is obtained by $\widehat{s}$, and then the reconstructed signal $\widehat{x}$ is obtained by the sparse transformation relation $x = \Psi s$.

3.2. **MIMO radar positioning model.** The MIMO radar emits orthogonal signals from N_T emitters. After the target is scattered by the target, some signals are received by N_R receiving array elements. Due to the orthogonal relationship between the emission waveforms, a plurality of transmit signals in the space can maintain their independence, so from the transmitting array to the receiving array has formed $N_T N_R$ channels in the air, each channel corresponds to a specific emission element to the target, the target path to a specific combination of array element. The delay of the channel is related to the location of the target and the transmitter. Figure 3 is shown as a simple model for MIMO radar positioning.

It is assumed that the space object is an ideal point, and the two-dimensional plane of the target is regarded as a grid structure. The word grid is derived from the geographic information system. The grid data structure is a simple and intuitive spatial data structure, also known as the grid data structure. If the ground is divided into $L = m \times n$ small squares, the location of each small square is known. At this time, whether there is a target object in the small square, it can be expressed by the matrix (the matrix element is 1, indicating that the target exists, and the

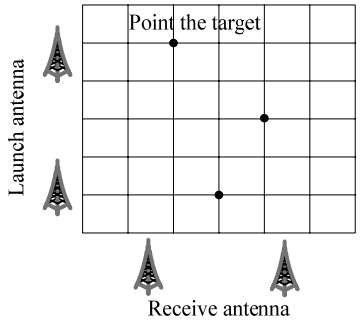

FIGURE 3. MIMO radar model

element is 0, indicating that there is no target object).According to this idea, the space of the object is taken as a plane, the plane is divided into a grid, and the target is locked in a grid.

The MIMO radar emits multiple orthogonal linear frequency modulation signals at the emitter. Supposing that the narrow band FM signal launched at the transmitter i is $x_i(t)$ and the mathematical expressions are formulated.

$$x_i(t) = u(t) \exp\left[j2\pi\left(\frac{1}{2}\mu t^2 + if_p t\right)\right] \tag{19}$$

Where, $\mu = B/T$ is the chirp rate, $f_p = 1/T$, B is the signal bandwidth, T is the pulse time, j is the imaginary unit. The signal is transmitted in the air, and it is reflected back to the receiving end after encountering the target. $\sigma_{ijk}(t)$ is defined as the attenuation coefficient of the i th transmitters that reflect back to jth receivers through kth target. τ_{ijk} is the signal delay, the formula is as follows:

$$\tau_{ijk} = \frac{1}{c}(|P_k - T_i| + |P_k + R_j|) \tag{20}$$

Where, c is the speed of light ($c = 3 \times 10^8 m/s$), P_k, T_i and T_j represent the coordinates of the target, the transmitting antenna and the receiving antenna. The signals of K targets are shown as formula (21) from ith emitter to jth receiving end.

$$y_{ij}(t) = \sum_{k=1}^{K} \sigma_{ijk}(t) x_i(t - \tau_{ijk}) = \sum_{k=1}^{K} \sigma_{ijk}(t) u(t) e^{j2\pi\left[\mu(t-\tau_{ijk})^2 + f_p(t-\tau_{ijk})\right]} \tag{21}$$

It is defined that a target state space is discrete into a grid of L values, which is represented as $\left\{\xi^l, 1, \ldots, L\right\}$. In case of the effect of the target state, let $\psi_{ijk}(n) = u(n)e^{j2\pi\left[\mu(t-\tau_{ijk})^2 + f_p(t-\tau_{ijk})\right]}$; otherwise, $\psi_{ijk}(n) = 0$. Similarly, if ξ^l is the state vector of the k th target, let $s_{ijl}(n) = \sigma_{ijl}(n)$; otherwise $s_{ijl}(n) = 0$. The element $s_{ijl}(n)$ and $\psi_{ijl}(n)$ are determined by four variables, as the four dimensional matrix and t $y_{ij}(n)$ is the three-dimensional matrix. The following elements is ordered as the order of different emitting end to the same receiving end, that is:

$$y(n) = [y_{11}(n), \ldots, y_{N_T 1}(n), \ldots, y_{1N_R}(n), \ldots, y_{N_T N_R}(n)]^T \tag{22}$$

$$s_l(n) = [s_{11l}(n), \ldots, s_{N_T 1l}(n), \ldots, s_{1N_R l}(n), \ldots, s_{N_T N_R l}(n)]^T \tag{23}$$

$$\psi_l(n) = diag\left\{\psi_{11l}(n), \ldots, \psi_{N_T 1l}(n), \ldots, \psi_{1N_R l}(n), \ldots, \psi_{N_T N_R l}(n)\right\} \tag{24}$$

The matrices $y(n)$ and $s_l(n)$ are both $N_T N_R \times 1$ - dimensional and $\psi_l(n)$ is the $N_T N_R \times N_T N_R$ dimensional diagonal matrices. The number $l = 1, \ldots, L$ of states is replaced into $s_l(n)$ and $\psi_l(n)$, and arranged according to formula (25) and (26):

$$s(n) = [s_1(n), s_2(n), \ldots, s_L(n)]^T \tag{25}$$

$$\psi(n) = [\psi_1(n), \psi_2(n), \ldots, \psi_L(n)] \tag{26}$$

At this point, $s(n)$ is a $LN_T N_R \times 1$ dimensional matrix, and $\psi(n)$ is a $N_T N_R \times LN_T N_R$ dimensional matrix. Further, the sample point n is valued as $1, 2, \ldots, N$ in turn. Since $s(n)$ is the attenuation coefficient, it is independent of the sampling point n, only the values of the variables Y and ψ are arranged according to formula

(27) and (28), respectively.

$$Y = \left\{ [y(1)]^T, [y(2)]^T, \ldots, [y(N)]^T \right\}^T \tag{27}$$

$$\psi = \left\{ [\psi(1)]^T, [\psi(2)]^T, \ldots, [\psi(N)]^T \right\}^T \tag{28}$$

Finally, it can get the formula (29):

$$Y_{(NN_TN_R)\times 1} = \psi_{(NN_TN_R)\times(LN_TN_R)} s_{(LN_TN_R)\times 1} \tag{29}$$

4. **Experimental results and analysis.** Taking the ship as the example: the ship docked at the port of Xiamen, the AIS location information provided by the Shipping News Network (118°05.456'E, 24 °32.687'N); camera monitoring the ship's time is 15:21 on April 7, 2015, The geodetic Cartesian coordinates of the camera position is (−2733672.0788, 5121154.1042, 2633528.7008), the level of tilt angle is 25 °, vertical angle is −1 °, tilt angle is 0.2 °, focal length f is X23, f = 126. 51mm; the image point coordinate of the ship center in the image is (−2, −7). According to these data, the ship's probability coordinates are (118°05.578'E, 24°32.774'N). By comparing the calculated approximate position coordinate with the AIS position coordinate, the error between the calculated location and the actual position in longitude direction is 0.121', and the error in latitude direction is 0.086'. In the same way, the errors in the direction of latitude and meridian of other ships are calculated according to the above steps, as shown in Table 1 and Table 2.

The longitude range is from 118°05.4' to 118° 06', and latitude ranges from 24°32.5' to 24°33.6'. The computed locations and actual locations of 8 ships in Table 1 and Table 2 are represented by the solid circle p1, p2, p3, ..., p8, respectively. Arrows and hollow p1, p2, p3, ..., p8 are represented in turn. The distribution of the location of the target and the actual position are shown in Figure 4.

TABLE 1. test data table of the target location algorithm

Target		Ship 1	Ship 2	Ship 3	Ship 4
Algorithm	$\Phi(^\circ)$	32	39	31	29
parameters	$\omega(^\circ)$	−1	−1	−1	−1
	$\kappa(^\circ)$	0.2	0.2	0.2	0.2
	x(mm)	14	−16	−1	−23
	y(mm)	9	2	−9	−7
	f(mm)	148.51	155	148.51	133
	X_C(m)	−2734008.694	−2733672.0788	−2734008.694	−2733672.0788
	Y_C(m)	5120687.4680	5121154.1044	5120687.4680	5121154.1044
	Z_C(m)	2634082.8485	2633528.7010	2634082.8485	2633528.7010
Calculated coordinate		118°05.872'E, 24°33.109'N	118°05.572'E, 24°32.779'N	118°05.883'E, 24°33.112'N	118°05.586'E, 24°32.773'N
Actual coordinate		118°05.906'E, 24°33.055'N	118°05.493'E, 24°32.700'N	118°05.896'E, 24°33.050'N	118°05.464'E, 24°32.655'N
Error	Longitude/'	0.034	0.079	0.013	0.122
	Latitude/'	0.054	0.079	0.062	0.118

TABLE 2. test data table of the target location algorithm

Target		Ship 5	Ship 6	Ship 7	Ship 8
Algorithm	$\Phi(^\circ)$	21	24	25	25
parameters	$\omega(^\circ)$	-1	-1	-1	-1
	$\kappa(^\circ)$	0.2	0.2	0.2	0.2
	x(mm)	-7	-9	-11	-2
	y(mm)	-12	-11	-5	-5
	f(mm)	166	155	155	126.6
	X_C(m)	-2733672.0788	-2733672.0788	-2733672.0788	-2733672.0788
	Y_C(m)	5121154.1044	5121154.1044	5121154.1044	5121154.1044
	Z_C(m)	2633528.7010	2633528.7010	2633528.7010	2633528.7010
Calculated coordinate		118°05.587'E, 24°32.774'N	118°05.586'E, 24°32.775'N	118°05.583'E, 24°32.773'N	118°05.580'E, 24°32.776'N
Actual coordinate		118°05.594'E, 24°32.798'N	118°05.480'E, 24°32.676'N	118°05.427'E, 24°32.669'N	118°05.459'E, 24°32.690'N
Error	Longitude/'	0.007	0.106	0.156	0.121
	Latitude/'	0.024	0.099	0.104	0.086

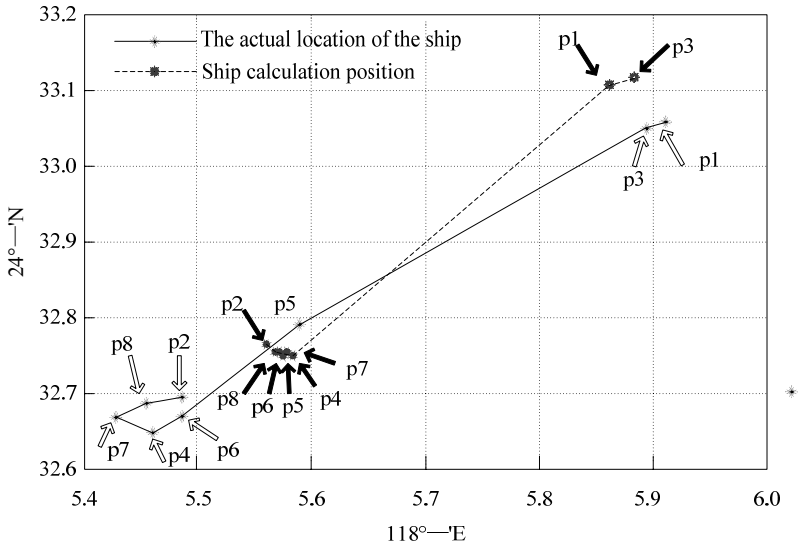

FIGURE 4. Comparison of the calculated position and the actual position of a ship

The error of the calculated longitude and the actual longitude of a ship is as shown in Figure 5. The diamond represents the actual longitude of the ship, and the triangle represents the calculated longitude of the ship. The error of the calculated latitude and the actual latitude of the ship is as shown in Figure 6. The diamond represents the actual latitude of the ship, and the triangle represents the calculated latitude of the ship.

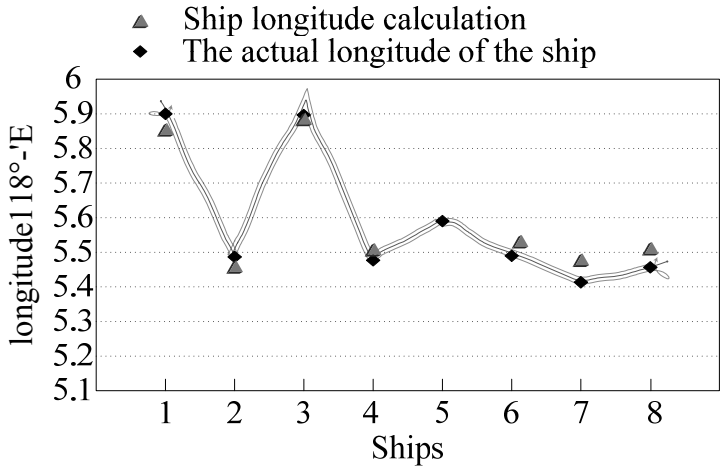

FIGURE 5. Comparison of calculate longitude and actual longitude of ship

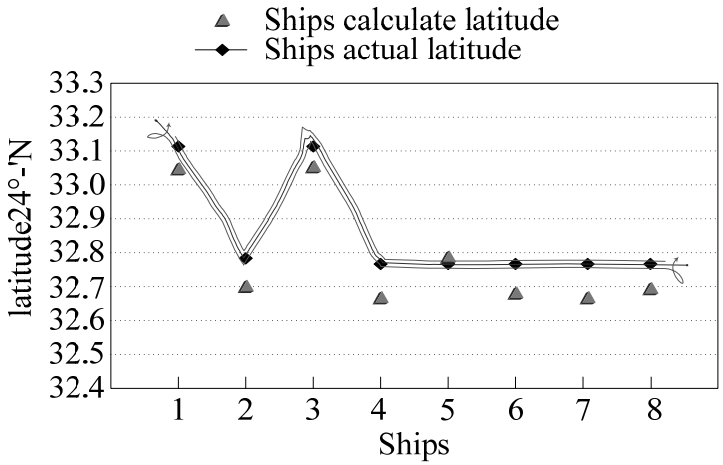

FIGURE 6. Comparison of the calculated latitudes and the actual latitudes of the ship

In Figure 5 and Figure 6, the average error of the calculated position and the actual position on the longitude is 148.163m, and the average error at latitude is 146.307m. The main sources of position error are coordinate transformation error, GPS positioning error, camera position and attitude measurement error, position difference of image points and GPS antenna. It is verified that the location error of moving target automatic tracking and localization algorithm is relatively small in complex environment, and the positioning accuracy can meet the accuracy requirements of maritime surveillance, search and rescue for maritime target location.

The automatic tracking algorithm and the target location algorithm based on curve fitting and based on wireless sensor network are used respectively for locating moving target test under complex environment. Time used of locating on the same

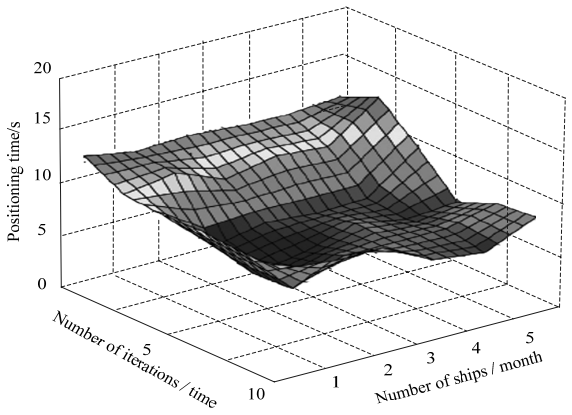

(a) the time used for location by the target location algorithm based on the wireless sensor network

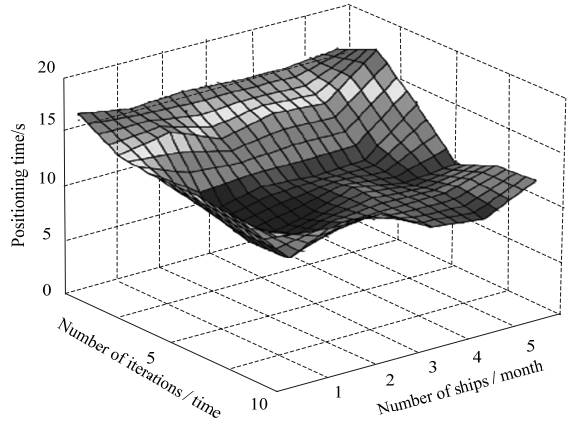

(b) the time used for location by the target location algorithm based on the curve fitting

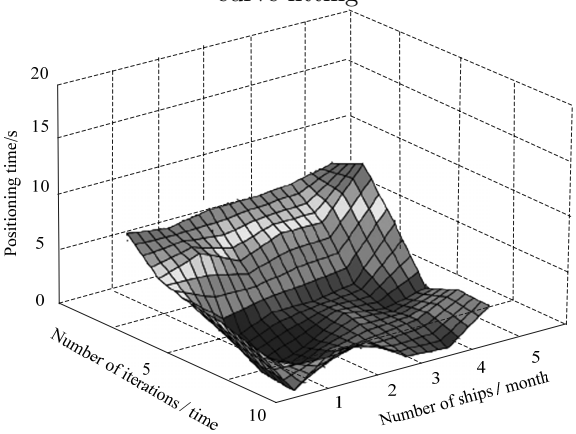

(c) the time used for positioning by the proposed method

FIGURE 7. the time used for positioning by the three different methods

target by three different methods are compared, and the test results are shown in figure 7.

Figure 7(a) and Figure 7(b) are the target location algorithms based on wireless sensor network and target location algorithm based on curve fitting respectively. Figure 7(c) is the time used to automatically track and locate the moving target by automatic tracking and positioning algorithm of moving target in complex environment. Figure 7(a), 7(b) and 7(c) show that the time of using the automatic tracking positioning algorithm for moving target under complex environment is less that that of the automatic tracking and positioning algorithm based on wireless sensor network and that based on curve fitting algorithm, indicating that the location of automatic tracking and positioning algorithm for moving target in complex environment is less time and more efficient.

5. **Conclusions.** Radar is an important weapon in national defense fighting and defense. It plays an important role in the military and plays a more and more important role in the large stage of civilian use. Locating targets is the most basic function of radar, especially in modern electronic warfare, precise location of targets is helpful for attacking enemy weapons accurately, and provides a powerful guarantee for destroying enemy planes accurately. At present, the moving target auto tracking and location algorithm takes a long time to locate the moving target in complex environment, and there is an error between the location result and the actual location of the target. In this paper, an automatic tracking and positioning algorithm for moving targets in complex environment is proposed, which can locate the moving target quickly and accurately in complex environment.

Acknowledgments. Aeronautical Science Fund (No. 20165852052);

The 13th five-year ministry of army equipment research project (No. 30102080 101).

REFERENCES

[1] A. H. Abdullah and et al., Mathematics teachers' level of knowledge and practice on the implementation of higher-order thinking skills (hots), *Eurasia Journal of Mathematics Science & Technology Education*, **13** (2016), 3–17.

[2] A. Ahadi and A. Dehghan, The inapproximability for the (0,1)-additive number, *Discrete Mathematics and Theoretical Computer Science*, **17** (2016), 217–226.

[3] F. Altinay-Gazi Zehra—Altinay-Aksal, Technology as mediation tool for improving teaching profession in higher education practices, *Eurasia Journal of Mathematics Science & Technology Education*, **13** (2017), 803–813.

[4] M. M. A. M. Aly and M. A. H. El-Sayed, Enhanced fault location algorithm for smart grid containing wind farm using wireless communication facilities, *Iet Generation Transmission & Distribution*, **10** (2016), 2231–2239.

[5] L. B. and L. W. S., Indoor positioning method based on cosine similarity of fingerprint matching algorithm, *Bulletin of Science and Technology*, **3** (2017), 198–202.

[6] T. P. S. Bains and M. R. D. Zadeh, Supplementary impedance-based fault-location algorithm for series-compensated lines, *IEEE Transactions on Power Delivery*, **31** (2016), 334–342.

[7] A. Basar and M. Y. Abbasi, On ordered bi–ideals in ordered-semigroups, *Journal of Discrete Mathematical Sciences and Cryptography*, **20** (2017), 645–652.

[8] T. Brough, L. Ciobanu, M. Elder and G. Zetzsche, Permutations of context-free, et0l and indexed languages, *Discrete Mathematics & Theoretical Computer Science*, **17** (2016), 167–178.

[9] J. Byrka, S. Li and B. Rybicki, Improved Approximation Algorithm for k-level Uncapacitated Facility Location Problem (with Penalties), *Theory Comput. Syst.*, **58** (2016), 19–44.

[10] Y. Cao, Optimal investment-reinsurance problem for an insurer with jump-diffusion risk process: correlated of brownian motions, *Journal of Interdisciplinary Mathematics*, **20** (2017), 497–511.
[11] M. Chen and C. X. Xu, Analysis of optimal utilization model of coastline resources in jiangsu province, *Journal of Interdisciplinary Mathematics*, **20** (2017), 1441–1444.
[12] P. S. Davis and T. L. Ray, A branch ound algorithm for the capacitated facilities location problem, *Naval Research Logistics*, **16** (2015), 331–344.
[13] W. Gao and W. Wang, A tight neighborhood union condition on fractional (g, f, n', m)-critical deleted graphs, *Colloquium Mathematicum*, **149** (2017), 291–298.
[14] W. Gao, L. Zhu, Y. Guo and K. Wang, Ontology learning algorithm for similarity measuring and ontology mapping using linear programming, *Journal of Intelligent & Fuzzy Systems*, **33** (2017), 3153–3163.
[15] Y. Gao, Optimization design of fast query system for retrieval information from large amount of books, *Modern Electronics Technique*, **9** (2016), 422–425.
[16] M. Ghorbani, An evolutionary algorithm for a new multi-objective location-inventory model in a distribution network with transportation modes and third-party logistics providers, *International Journal of Production Research*, **53** (2015), 1038–1050.
[17] R. J. Hamidi and H. Livani, Traveling-wave-based fault-location algorithm for hybrid multiterminal circuits, *IEEE Transactions on Power Delivery*, **32** (2017), 135–144.
[18] B. Hartke, Global cluster geometry optimization by a phenotype algorithm with niches: Location of elusive minima, and low rder scaling with cluster size, *Journal of Computational Chemistry*, **20** (2015), 1752–1759.
[19] T. Jin, Y. F. Niu and L. Zhou, Methods of evaluating cognitive performance of products digital interface, *Journal of Discrete Mathematical Sciences & Cryptography*, **20** (2017), 295–308.
[20] Z. Liu, M. Chao, J. Zhang, X. Zhang, Y. Liu and J. Zhang, Research on mathematical properties of localization algorithm based on sensor relative position in wsn, *Journal of Jilin University(Information Science Edition*, **6** (2015), 685–689.
[21] G. Preston, Z. M. Radojevic, C. H. Kim and V. Terzija, New settings-free fault location algorithm based on synchronised sampling, *Iet Generation Transmission & Distribution*, **5** (2015), 376–83.
[22] S. Sun, K. Dong, J. J. Xiu and Y. Liu, A passive source localization algorithm with multiple moving observers using tdoa/groa measurements based on cwls, *Journal of China Academy of Electronics & Information Technology*, **5** (2016), 540–546.
[23] Y. Sun, J. Qi, R. Zhang, Y. Chen and X. Du, Mapreduce based location selection algorithm for utility maximization with capacity constraints, *Computing*, **97** (2015), 403–423.
[24] P. H. Tseng and K. T. Lee, A femto-aided location tracking algorithm in lte-a heterogeneous networks, *IEEE Transactions on Vehicular Technology*, **66** (2017), 748–762.
[25] G. Weckman, Applying genetic algorithm to a new location and routing model of hazardous materials, *International Journal of Production Research*, **53** (2015), 916–928.
[26] W. Yi, Assessment study on brain wave predictive ability to policemen's safety law enforcement, *Journal of Discrete Mathematical Sciences and Cryptography*, **20** (2017), 193–204.
[27] J. J. Zhang and K. Qiang, Modeling of complex information system based on hierarchical decision-making theory, *Journal of Discrete Mathematical Sciences & Cryptography*, **20** (2017), 137–148.

Received June 2017; revised November 2017.

E-mail address: liurong8120@163.com
E-mail address: mhamdiara@yahoo.fr